

1 **Predicting plant immunity gene expression by identifying the decoding**
2 **mechanism of calcium signatures**

3
4
5
6 Gioia Lenzone, Junli Liu*, and Marc R. Knight*

7 Department of Biosciences, Durham University, South Road, Durham DH1 3LE, UK.

8
9 *Correspondence: MRK (email: m.r.knight@durham.ac.uk; tel: 0191 334 1224) and JL
10 (email: junli.liu@durham.ac.uk; tel: 0191 334 1376)

11
12
13
14
15 Brief heading: Mechanism of decoding calcium signatures

16
17
18
19
20
21 Total word count: 5786

22 Introduction word count: 800

23 Materials and Methods word count: 1267

24 Results word count: 2160

25 Discussion word count: 1553

26 Acknowledgements word count: 15

27 Total number of figures: 6

28 Number of figures to be published in colour: 5

29 Supplementary tables: 2

30 Supplementary figures: 8

31

32 **Summary**

33 • Calcium plays a key role in determining the specificity of a vast array of signalling
34 pathways in plants. Cellular calcium elevations with different characteristics (calcium
35 signatures) carry information on the identity of the primary stimulus, ensuring appropriate
36 downstream responses. However, the mechanism for decoding calcium signatures is
37 unknown. To determine this, decoding of the SA-mediated plant immunity signalling
38 network controlling gene expression was examined.

39 • A dynamic mathematical model of the SA-mediated plant immunity network was
40 developed. This model was used to predict responses to different calcium signatures; these
41 were validated empirically using quantitative real-time PCR to measure gene expression.

42 • The mechanism for decoding calcium signatures to control expression of plant
43 immunity genes *EDS1* and *ICS1* was identified. Calcium, calmodulin, CAMTA3 and CBP60g
44 together amplify each calcium signature into three active signals, simultaneously regulating
45 expression. The time required for calcium to return to steady-state level also quantitatively
46 regulates gene expression.

47 • Decoding of calcium signatures occurs via nonlinear interactions between these
48 active signals, producing a unique response in each case. Key properties of the calcium
49 signatures are not intuitive, exemplifying the importance of mathematical modelling
50 approaches. This approach can be applied to identifying the decoding mechanisms of other
51 plant calcium signalling pathways.

52

53 **Keywords**

54 calcium signalling, gene expression, modelling, plant immunity, specificity, decoding,
55 salicylic acid.

56

57 **Introduction**

58 The second messenger calcium plays a key role in the specificity of signalling pathways in
59 eukaryotes as it controls a vast array of cellular responses (Berridge *et al.*, 2003; Clapham,
60 2007). Interestingly, different primary stimuli lead to cellular calcium elevations with
61 different kinetics, each distinct calcium elevation being termed a “calcium signature”
62 (McAinsh & Pittman, 2009). Of key importance is that information in the form of calcium
63 signatures is used by cells to specify the nature and severity of the primary stimulus
64 (McAinsh & Pittman, 2009; Ranty *et al.*, 2016). Thus, calcium signatures encode specific

65 information that can be decoded by cells to elicit the appropriate response; *e.g.* recognition
66 of plant pathogenic and symbiotic microbes (Zipfel & Oldroyd, 2017), expression of stress
67 genes in plants (Whalley & Knight, 2013) and closure of guard cells (Allen *et al.*, 2001).
68 Without the correct calcium signature, the plant does not activate the appropriate response
69 to a given stress, and therefore does not adapt to the new condition, affecting its fitness to
70 survive. The specific information carried by calcium signatures is relayed to the end
71 response via calcium-binding proteins: the “decoders” (Hashimoto & Kudla, 2011). In the
72 case of regulation of gene expression specifically, we have previously shown that different
73 calcium signatures can regulate different genes, by controlling different transcription factors
74 (Whalley & Knight, 2013). For one specific case, the calmodulin-binding transcription
75 activators transcription factors (CAMTA), we developed a model to explain the differential
76 activation of these transcription factors in response to different calcium signatures (Liu *et*
77 *al.*, 2015).

78 The fundamental question of how specific calcium signatures are decoded to
79 produce the correct appropriate response, however, is not yet known. In this paper we take
80 a combined modelling and experimental approach to answer this question using the
81 expression of genes involved in salicylic acid (SA) regulated plant immunity as an example. It
82 has been demonstrated that increases in calcium, and the calcium binding proteins
83 responding to these increases in calcium, are necessary for plant immunity (Kim *et al.*, 2002;
84 McAinsh & Pittman, 2009; Dodd *et al.*, 2010; Galon *et al.*, 2010; Kudla *et al.*, 2010; Seybold
85 *et al.*, 2014; Tsuda & Somssich, 2015). One of the primary roles of calcium signalling in plant
86 immunity is the regulation of SA biosynthesis (Zhang *et al.*, 2010; Zhang *et al.*, 2014). SA is a
87 phytohormone that plays a central role in plant defence signalling (Vlot *et al.*, 2009),
88 specifically regulating the changes in nuclear gene expression which are required for
89 activating plant resistance. Calcium has been demonstrated empirically to play a very
90 prominent role in controlling the plant immune response (Kim *et al.*, 2009; Seybold *et al.*,
91 2014) including SA biosynthesis. In particular, different calcium-associated transcription
92 factors, such as CAMTA3 (AtSR1) and CBP60g, regulate gene expression in plant immunity
93 (Zhang *et al.*, 2010; Zhang *et al.*, 2014). CAMTA3 and CBP60g are well characterised
94 Ca²⁺/calmodulin (CaM)-regulated transcription factors and both have a CaM binding domain
95 (Finkler *et al.*, 2007; Galon *et al.*, 2008; Kim *et al.*, 2009; Wang *et al.*, 2009; Zhang *et al.*,
96 2010; Reddy *et al.*, 2011; Wang *et al.*, 2011; Bickerton & Pittman, 2012; Poovaiah *et al.*,

97 2013). Several genes involved in mediating plant immunity are regulated by these
98 transcription factors. For example, *EDS1* (*enhanced disease susceptibility 1*), part of the SA
99 network, was reported to be directly regulated by AtSR1 (CAMTA3) (Du *et al.*, 2009).
100 Expression of *ICS1* (*isochorismate synthase 1*) is similarly regulated by CBP60g (Wang *et al.*,
101 2009; Zhang *et al.*, 2010; Wang *et al.*, 2011) and *ICS1* encodes a key enzyme in salicylic acid
102 (SA) production (Zhang *et al.*, 2010). Expression of these genes thus plays a key role in plant
103 immunity by regulating the levels of the plant defence hormone salicylic acid (Zhang *et al.*,
104 2010; Zhang *et al.*, 2014). Therefore, in this way, calcium plays a pivotal role in fine-tuning
105 SA biosynthesis through the simultaneous positive regulation of *ICS1* (promoting SA
106 production) and *EDS1* (which is a positive regulator of *ICS1*) during response to pathogens.

107 Whilst it is known that Ca^{2+} signals are of key importance for the activation of plant
108 immunity (Kim *et al.*, 2002; McAinsh & Pittman, 2009; Dodd *et al.*, 2010; Galon *et al.*, 2010;
109 Kudla *et al.*, 2010; Seybold *et al.*, 2014; Tsuda & Somssich, 2015), and that different calcium
110 signatures are generated in response to different microbial pathogens (Grant *et al.*, 2000), it
111 is not yet known how the signatures are decoded by cells to produce the appropriate
112 specific gene expression pattern essential for immunity. It is to answer this intriguing
113 question that the research presented here is aimed. The mathematical model we developed
114 as a consequence was able to predict patterns of *ICS1* and *EDS1* gene expression in response
115 to different calcium signatures, which were validated empirically. This approach can be
116 applied to identifying the decoding mechanisms of other plant calcium signalling pathways.

117

118 **Materials and Methods**

119 **Plant materials, growth conditions and treatments with calcium agonists.** Experiments
120 were performed on transgenic *Arabidopsis thaliana* L. (Heyn) lines constitutively expressing
121 35S::apoequorin in the cytosol (pMAQ2, Col-0 ecotype, (Knight *et al.*, 1991)). Seeds were
122 ethanol-sterilised, sown on 1 X Murashige and Skoog (MS, Duchefa Biochemie) medium pH
123 5.8 (Murashige & Skoog, 1962), 0.8% (w/v) agar (Sigma-Aldrich) on Petri dishes, stratified for
124 a minimum of 48 h at 4°C before growing them at 20°C with a 16/8 h photoperiod at a light
125 intensity of $150 \mu\text{mol m}^{-2} \text{s}^{-1}$. Calcium measurements and agonist treatments were
126 performed on 8-day-old seedlings; aequorin reconstitution was performed on 7-day-old
127 seedlings. For all the chemical treatments, 7 day-old *Arabidopsis* seedlings were floated in

128 water in the dark overnight (Knight & Knight, 1995). The next day seedlings were transferred
129 to a luminometer cuvette (Röhren), and after a 30 minutes resting period the agonist was
130 injected at double concentration, both for calcium experiments and for gene expression
131 measurements. To test for differential transcript levels, plants were treated with the
132 chemicals for 1h, 3h, 6h and 9h. The final concentration of the calcium agonists tested were
133 500 μ M ATP, 1 mM L-glutamate, 50 mM calcium (II) chloride and 10 μ M mastoparan (all
134 from Sigma-Aldrich). For each of the agonists at each timepoint batches of 5 seedlings were
135 chemically treated inside a luminometer cuvette after a 30 min resting period, to exactly
136 emulate conditions used for the calcium measurements. For each sample for gene
137 expression analysis (representing one agonist at one timepoint), 3 separate biological
138 replicates (15 seedlings in total) were pooled before RNA extraction. The whole experiment
139 (involving 4 agonists plus baseline, at 4 different timepoints) was performed twice and data
140 presented are averages of these 2 separate experiments.

141 ***In vivo* reconstitution of aequorin and Ca²⁺-dependent luminescence measurements.**
142 Aequorin reconstitution was performed by floating *Arabidopsis* seedlings on water
143 containing 10 μ M coelenterazine 1% [v/v] methanol (Biosynth). Plants were left in the dark
144 from 12 to 24 h at 20°C before calcium measurements. To measure calcium levels,
145 *Arabidopsis* seedlings were transferred to a luminometer cuvette and inserted into the
146 luminometer sample housing. Following a 30 min resting period, luminescence levels were
147 recorded every 1 sec using a digital chemiluminometer with discriminator and cooled
148 housing unit (Electron Tubes Limited). Luminescence was recorded for 120 sec before
149 injection of the chemical to provide baseline steady-state readings. Discharge was
150 performed at the end of the experiment by injection of an equal volume of 2 M CaCl₂, 20%
151 ethanol. Calibration was performed as previously described (Knight *et al.*, 1996).

152 **cDNA preparation and gene expression measurements.** A high capacity cDNA reverse
153 transcription kit (Applied Biosystem) was used to reverse transcribe 2 μ g of total RNA
154 obtained with a RNeasy Plant Total RNA kit (Qiagen). Quantitative real-time PCR was
155 performed on 5 μ L of 1:50 cDNA dilution in a total volume of 15 μ L, using an Applied
156 Biosystem 7300 real time PCR machine. Relative expression levels of *EDS1* (At3g48090) and
157 *ICS1* (At1g74710) were tested with Fast Start SYBR Green Master Mix with ROX using the
158 following primers: *EDS1* Fw 5'-ACCTAACCGAGCGCTATCAC-3', *EDS1* Rev 5'-

159 TTGTCCGGATCGAAGAAATC-3', *ICS1* Fw 5'-CAAATCTCAACCTCCGTCGT-3', *ICS1* Rev 5'-
160 AATCAATTGCTCCGATTGTC-3'. Levels were normalised to the endogenous levels of the *PEX4*
161 housekeeping gene (At5g25760), and the primers used were *PEX4* Fw 5'-
162 TCATAGCATTGATGGCTCATCCT-3', *PEX4* Rev 5'-ACCCTCTCACATCACCAGATCTTAG-3'.
163 Experiments were performed in optical 96-well plates, with eight technical replicates for
164 each sample. Relative quantification was performed by the $\Delta\Delta C_t$ method (Livak &
165 Schmittgen, 2001), the values obtained representing the relative quantitation (RQ)
166 estimates, and the error bars, representing RQ_{MAX} and RQ_{MIN} , were calculated as described
167 previously (Knight *et al.*, 2009). The algorithm used is described in Relative Quantitation
168 (RQ) Algorithms in Applied Biosystems Real-Time PCR Systems Software (Applied Biosystems
169 Real-Time PCR Systems, 2007).

170 **Differential equations for modelling gene expression.** MNNCC_ described in the text is
171 referred to as MNNCCb in the following equations for the clarity of notation. Both b in the
172 equations and _ in the text refer to no binding of any protein to CaM.

$$173 \frac{d[mRNA_{EDS1}]}{dt} = \frac{V_{EDS1}^{max} \frac{[MNNCCb]}{k_{EDS1,MNNCCb}} \frac{[DR]}{k_{EDS1,DR}}}{\left(1 + \frac{[MNNCCb]}{k_{EDS1,MNNCCb}}\right) \left(1 + \frac{[DR]}{k_{EDS1,DR}}\right) \left(1 + \frac{[MNNCCX]}{k_{EDS1,MNNCCX}}\right)} - k_{EDS1,decay} [mRNA_{EDS1}] \quad (\text{eq.1})$$

$$174 \frac{d[mRNA_{ICS1}]}{dt} = \frac{V_{ICS1}^{max} \frac{[MNNCCY]}{k_{ICS1,MNNCCY}} \frac{[mRNA_{EDS1}]}{k_{ICS1,MNNCCb}} \frac{[DR]}{k_{ICS1,DR}}}{\left(1 + \frac{[MNNCCY]}{k_{ICS1,MNNCCY}}\right) \left(1 + \frac{[mRNA_{EDS1}]}{k_{ICS1,MNNCCb}}\right) \left(1 + \frac{[DR]}{k_{ICS1,DR}}\right)} - k_{ICS1,decay} [mRNA_{ICS1}] \quad (\text{eq.2})$$

$$175 \frac{d[DR]}{dt} = \frac{V_{DR}^{max} \frac{[mRNA_{ICS1}]}{k_{DR,ICS1}}}{\left(1 + \frac{[mRNA_{ICS1}]}{k_{DR,ICS1}}\right)} - k_{DR,decay} [DR] \quad (\text{eq.3})$$

176 $[mRNA_{EDS1}]$ and $[mRNA_{ICS1}]$ are the transcript concentration of *EDS1* and *ICS1*,
177 respectively. $[DR]$ is the concentration of *ICS1* downstream. $[MNNCCb]$, $[MNNCCX]$
178 and $[MNNCCY]$ are the concentration of the active complexes of calcium signals, $4Ca^{2+}$ -
179 CaM, $4Ca^{2+}$ -CaM-CAMTA3 and $4Ca^{2+}$ -CaM-CBP60g, respectively. $k_{EDS1,MNNCCX}$ is the binding

180 affinity of CAMTA3 to DNA for *EDS1* gene expression. All other $k_{\alpha,\beta}$ symbols in the first
181 term of equations 1-3 have the same meaning. $k_{EDS1,decay}$, $k_{ICS1,decay}$ and $k_{DR,decay}$ are the first-
182 order decay rate for $mRNA_{EDS1}$, $mRNA_{ICS1}$ and *DR*, respectively. $[MNNCCb]$, $[MNNCCX]$
183 and $[MNNCCY]$ are computed using the upper pane of Fig. 3. The binding of CAMTA3 with
184 calmodulin and Ca^{2+} generates 33 binding reactions and 18 different binding complexes<sup>(Liu et
185 al., 2015)</sup>. Following the analysis previously developed (Liu et al., 2015), the binding of both
186 CAMTA3 and CBP60g with calmodulin and Ca^{2+} generates 54 binding reactions and 27
187 different binding complexes. In addition, there are a large number of different Ca^{2+} /CaM
188 binding proteins (Reddy et al., 2011; Poovaiah et al., 2013) in plant cells. In addition to
189 CAMTA3 and CBP60g, any other calmodulin binding proteins or transcription factors can be
190 included in the model. Because other calmodulin binding proteins or transcription factors
191 can compete for the binding of calmodulin, they affect the concentrations of the active
192 complexes of calcium signals, $4Ca^{2+}$ -CaM, $4Ca^{2+}$ -CaM-CAMTA3 and $4Ca^{2+}$ -CaM-CBP60g.
193 Therefore, different numbers of other calmodulin binding proteins or transcription factors
194 affect the searched parameter values. The parameters shown in Table S1 corresponds to
195 100 other calmodulin binding proteins or transcription factors in the model. For the sake of
196 simplicity and due to the lack of biological knowledge on other calmodulin binding proteins,
197 we consider that these 100 other calmodulin binding proteins or transcription factors have
198 the same binding affinity with calmodulin and they have the same concentration. How the
199 other parameters are searched is included in Table S1.

200

201 **Numerical Method.** The model was implemented using simulator Berkeley Madonna
202 (www.berkeleymadonna.com). Rosenbrock (Stiff) method was used with a tolerance of
203 $1.0e-5$. Much smaller tolerances ($1.0e-6$ to $1.0e-8$) were also tested and the numerical
204 results show that further reduction of tolerances did not improve the accuracy of numerical
205 results. To study how a calcium signature induces gene expression, the system of ordinary
206 differential equations was settled at a steady state using the average Ca^{2+} concentration of
207 the control experiment as an input before a calcium signature was introduced. Thus, the
208 steady-state values of all concentrations computed using the average Ca^{2+} concentration of
209 the control experiment as an input are the initial values of all concentrations, as shown in

210 the computational code, Table S2. When a calcium signature was introduced, the response
211 of the system of ordinary differential equations was calculated using the experimentally
212 measured time-dependent Ca^{2+} concentration (Fig. 1) as an input.

213 Since this work studies how a calcium signature induces gene expression, the initial values
214 of all concentrations are set to be the steady-state values corresponding to the Ca^{2+}
215 concentration of the control experiment. During the model development, we tested the
216 effects of initial values on modelling results. For the model parameters described in Table S1
217 and using the average Ca^{2+} concentration of the control experiment as an input, the
218 interactions of Ca^{2+} , CaM, CAMTA3, CBP60g and 100 other proteins establish a steady state
219 very quickly (<10s) from any initial value. Thus, modelling results are similar for all initial
220 values for these interactions. However, for the gene expression described by eq.1, 2 and 3,
221 response of gene expression to a calcium signature depends on initial values, and therefore
222 the initial values in eq. 1, 2 and 3 must be set to be the respective steady-state values using
223 the average Ca^{2+} concentration of the control experiment as an input.

224

225 **Results**

226 **Using the calcium agonist mastoparan to establish the relationship between different** 227 **calcium signatures and specific gene expression responses.**

228 To initially establish the relationship between calcium signatures and calcium-dependent
229 gene expression, we treated Arabidopsis seedlings with the known calcium agonist
230 mastoparan (Fig. 1a,b). Calcium measurements were performed using the recombinant
231 aequorin method (Knight & Knight, 1995). The genes *EDS1* and *ICS1* encode key components
232 of the salicylic acid biosynthetic pathway, required for response to pathogens (Zhang *et al.*,
233 2010; Zhang *et al.*, 2014). We therefore initially tested the effect of the calcium signature
234 generated by mastoparan upon *EDS1* and *ICS1* transcript expression levels which were
235 quantified by using real-time PCR (Fig. 2). Mastoparan treatment induced *ICS1* gene
236 expression at 3 hours by approximately 37 fold (Fig. 2a) whereas the same treatment only
237 induced a much more modest (approximately 2-3 fold) increase in *EDS1* gene expression
238 (Fig. 2b). The kinetics of expression were also different in both cases, for *ICS1* expression
239 peaked already at 3h and declined relatively slowly until 9h. In contrast, for *EDS1*, maximal
240 induction was achieved at 3h, declining again by 6h. We then used these data to elucidate of

241 the relationship between calcium signatures and expression responses of *EDS1* and *ICS1* by
242 modelling the information flow from calcium signals to *EDS1* and *ICS1* gene expression.

243

244 **A dynamic model for the information flow from calcium signals to gene expression.**

245 Experimental data accumulated over many years have shown that expression of *EDS1* and
246 *ICS1* is regulated by the transcription factors CAMTA3 and CBP60g, respectively (Du *et al.*,
247 2009; Wang *et al.*, 2009; Zhang *et al.*, 2010; Wang *et al.*, 2011). In addition, it has been
248 established experimentally that there is a regulatory network involving *EDS1* and *ICS1*
249 expression as well as their downstream response (Zhang *et al.*, 2014). In this network, *EDS1*
250 and *ICS1* expression and their downstream response are all mutually regulated. Specifically,
251 *EDS1* expression is positively regulated by both *EDS1* upstream and *ICS1* downstream, but it
252 is negatively regulated by the CAMTA3 transcription factor (Zhang *et al.*, 2014). *ICS1*
253 expression is promoted by *EDS1* expression since *EDS1* is an upstream component of *ICS1*
254 expression (Zhang *et al.*, 2014). *ICS1* expression is also positively regulated by both *ICS1*
255 downstream and the CBP60g transcription factor (Zhang *et al.*, 2014). Since both CAMTA3
256 and CBP60g have CaM binding domains, it has been demonstrated that Ca²⁺ signals regulate
257 the network of *EDS1* and *ICS1* expression and their downstream response (Zhang *et al.*,
258 2014). Taking all these facts into account, Fig. 3 summarises the dynamical model for
259 establishing information flow from calcium signals to *EDS1* and *ICS1* gene expression.

260 The model shown in Fig. 3 includes the fact that CAMTA3 has a calmodulin binding
261 site (Finkler *et al.*, 2007). Since CaM has two pairs of Ca²⁺-binding EF-hand domains located
262 at the N-and C-terminus respectively, interactions of Ca²⁺-CaM generate 9 different binding
263 complexes via 12 elementary binding processes, and interactions of Ca²⁺-CaM and CAMTA3
264 generate 18 different binding complexes via 33 elementary binding processes (Liu *et al.*,
265 2015). Similarly, interactions between Ca²⁺-CaM and CBP60g also generate 18 different
266 binding complexes, 9 of which are Ca²⁺-CaM only complexes and are the same as those in
267 interactions of Ca²⁺-CaM and CAMTA3. Therefore, 9 new complexes are generated for
268 interactions between Ca²⁺-CaM and CBP60g. In addition, plant cells contain a relatively
269 large number of other Ca²⁺/CaM binding proteins (Reddy *et al.*, 2011; Poovaiah *et al.*, 2013),
270 and these must be taken into account as they compete with CAMTA3 and CBP60g for CaM.
271 Each of these Ca²⁺/CaM binding proteins can be analysed using the same method developed
272 for interactions of Ca²⁺-CaM and CAMTA3 (Liu *et al.*, 2015). For each additional CaM binding

273 protein, 9 new binding complexes are generated. Thus, for n CaM binding proteins there are
274 $9(n+1)$ binding complexes. Published experimental measurements have shown that 4Ca^{2+} -
275 CaM is the active CaM- Ca^{2+} binding complex (Piffl *et al.*, 1984). Therefore, our model
276 assumes that the 4Ca^{2+} -CaM-TF complex is the active complex for gene expression
277 responses (Piffl *et al.*, 1984; Liu *et al.*, 2015). Thus, for CAMTA3 and CBP60g, the active
278 complexes for gene expression response are assumed to be 4Ca^{2+} -CaM-CAMTA3 and 4Ca^{2+} -
279 CaM-CBP60g, respectively.

280 The regulatory network upstream of *EDS1* gene is composed of many components,
281 which are regulated by Ca^{2+} signals (Zhang *et al.*, 2014). *EDS1* expression is promoted by the
282 upstream part of this network (Zhang *et al.*, 2014). For model development, we simplified
283 the regulation of *EDS1* gene expression by the upstream components into a single
284 regulatory relationship that is the activation of *EDS1* gene expression by Ca^{2+} signals. Since
285 experimental measurements have shown that 4Ca^{2+} -CaM is the active CaM and Ca^{2+} binding
286 complex (Piffl *et al.*, 1984), we assume the 4Ca^{2+} -CaM complex is the active signal that
287 positively regulates *EDS1* gene expression from the upstream part of the network (Zhang *et al.*
288 *et al.*, 2014). In addition, we simplified the network downstream of *ICS1* into a single response
289 component, DR (downstream response). The transcription factor CAMTA3 inhibits *EDS1*
290 gene expression, and DR activates *EDS1* gene expression (Zhang *et al.*, 2014). The expression
291 of *ICS1* is positively-regulated by *EDS1*, CBP60g transcription factor and DR (Zhang *et al.*,
292 2014). Thus, the interaction of *EDS1*, *ICS1* and DR forms the regulatory network shown in
293 Fig. 3.

294 Fig. 3, therefore, describes the information flow from calcium signatures to *EDS1* and
295 *ICS1* gene expression. The complexity of this information transduction process is
296 multifaceted. Our model (Fig. 3) has included the following aspects. Firstly, transient
297 changes of Ca^{2+} concentration are converted into transient active complexes following the
298 stoichiometry and binding mechanism of Ca^{2+} , CaM, CAMTA3 and CBP60g. Secondly, a large
299 number of other CaM-binding proteins can also bind with CaM. We have included the
300 effects of other CaM-binding proteins in our model. Thirdly, the interaction of *EDS1*, *ICS1*
301 and DR forms a regulatory network. Fourthly, after being converted into the 3 active
302 complexes of (1) 4Ca^{2+} -CaM; (2) 4Ca^{2+} -CaM-CAMTA3 and (3) 4Ca^{2+} -CaM-CBP60g, Ca^{2+} signals
303 have multiple effects on the *EDS1* and *ICS1* expression by regulating the network upstream
304 of *EDS1* and the CAMTA3 and CBP60g transcription factors. Thus, when a calcium signature

305 occurs, transient changes of Ca^{2+} concentration dynamically regulate the response of *EDS1*,
306 *ICS1* and DR in a complex and nonlinear manner. The dynamic model (Fig. 3) integrates a
307 wide range of knowledge about the information flow from Ca^{2+} signatures to expression of
308 *EDS1* and *ICS1*. To establish the parameters of this model, we compared the output of the
309 model in terms of mastoparan-induced *EDS1* and *ICS1* expression responses to our
310 experimental observations of gene expression (Fig. 2a,b).

311

312 **Modelling results reproduce experimental observations.**

313 Fig. 5 shows an example of fitting the dynamic model (Fig. 3) to the experimentally
314 measured transcript fold changes for both *EDS1* and *ICS1* genes (Fig. 2) in response to the
315 calcium signature induced by 10 μM mastoparan (Fig. 1a,b). For the unmeasured Ca^{2+}
316 concentration, we assume that Ca^{2+} concentration approaches the original steady state (Fig.
317 4a). For simplicity, we consider that Ca^{2+} concentration linearly decreases to its steady state
318 within τ_c (Fig. 4a), defined as the time required for a calcium signature to return to its
319 steady state. For different values of τ_c , Fig. 4b,c,d show the responses of the
320 concentrations of the three active complexes ($4\text{Ca}^{2+}\text{-CaM-CAMTA3}$, $4\text{Ca}^{2+}\text{-CaM-CBP60g}$ and
321 $4\text{Ca}^{2+}\text{-CaM}$, respectively). Importantly, Fig. 5a,b show that, although different values of τ_c
322 always generate similar temporal trends for transcript fold changes for both *EDS1* and *ICS1*,
323 different values of τ_c do quantitatively affect modelling results. In Fig. 5, the values of τ_c in
324 the range of 2-3 hours generate results which best fit to experimental observations.
325 Therefore, Fig. 4 and Fig. 5 reveals how the calcium signature induced by 10 μM mastoparan
326 is decoded to generate specific responses of *EDS1* and *ICS1* expression. When the
327 mastoparan calcium signature is produced, the transient elevation in intracellular Ca^{2+}
328 concentration is converted into three active complexes that regulate *EDS1* and *ICS1*
329 expression: $4\text{Ca}^{2+}\text{-CaM}$, $4\text{Ca}^{2+}\text{-CaM-CAMTA3}$ and $4\text{Ca}^{2+}\text{-CaM-CBP60g}$. (Fig. 3). For the
330 calcium signature induced by 10 μM mastoparan (Fig. 1a,b), transient elevation in
331 intracellular Ca^{2+} concentration is limited to a relatively small range and the maximum fold
332 change relative to the steady-state Ca^{2+} concentration is less than 10 fold during the lifetime
333 of this calcium signature (Fig. 1a,b). However, due to the action of CaM, CAMTA3 and
334 CBP60g in decoding this calcium signature (Fig. 3), the three active complexes ($4\text{Ca}^{2+}\text{-CaM}$,
335 $4\text{Ca}^{2+}\text{-CaM-CAMTA3}$ and $4\text{Ca}^{2+}\text{-CaM-CBP60g}$) vary their concentrations by a much wider

336 range and the maximum fold changes relative to their steady-state values and can reach
337 around 2500 fold. Thus, one calcium signature is amplified into three active signals and each
338 of these three amplified signals is capable of regulating *EDS1* or *ICS1* expression response
339 (Fig. 3). In addition, since expression of *EDS1* and *ICS1* forms a network (Fig. 3), the three
340 active signals, which originate from the same calcium signature, interplay via this network.
341 Thus, regulation of *EDS1* and *ICS1* expression by the mastoparan-induced calcium signature
342 (Fig. 5a,b) is highly nonlinear due to these interactions of the three amplified active signals
343 (Fig. 4b,c,d). Since the dynamic model (Fig. 3) can reproduce experimental data, we
344 conclude that the model captures the main features of the information flow from calcium
345 signals to *EDS1* and *ICS1* gene expression.

346 The next step was to test whether, now that it was established and parameterised,
347 the model could predict *EDS1* and *ICS1* gene expression responses to other calcium
348 signatures (Fig. 1), as gauged by comparing model-derived predictions to empirically-
349 determined gene expression data.

350

351 **Predictions of how three different calcium signatures will be decoded match empirical** 352 **observations of gene expression responses.**

353 To predict the relationships between calcium signatures and gene expression responses we
354 used the other three experimentally measured calcium signatures induced by treatments
355 with the calcium agonists ATP, extracellular calcium and glutamate (Fig. 1). These
356 empirically-derived calcium signatures were used, as model inputs, to calculate the
357 predicted transcript fold responses for both *EDS1* and *ICS1* gene expression without
358 changing any parameters (Fig. 6a,b,c,d,e,f). As Ca^{2+} concentrations of different calcium
359 signatures at the end of the experimentally measured data are different (Fig. 1), it is
360 plausible that different calcium signatures may have different values of τ_c . Thus, we
361 generated predictions for a range of τ_c values. Fig. 6 shows that the modelling predictions
362 on the transcript fold responses for both *EDS1* and *ICS1* to the 3 calcium signatures (Fig. 1)
363 are in agreement with experimental fold changes and temporal trends. Experimental data
364 show that whilst a 10 μM mastoparan treatment induced large fold change in *ICS1* gene
365 expression (around 37 fold at 3 hours, Fig. 2a) the other three calcium signatures could only
366 induce much smaller fold changes in *ICS1* gene expression (approximately maximum 5 fold

367 at 6 hours, Fig. 6a). As can be seen in Fig. 6a,c,e the model indeed predicts that the other
368 three calcium signatures in Fig. 1 would indeed only generate relative small fold change for
369 *ICS1* expression (around maximum 5 fold at 6 hours (see the curve corresponding to $\tau_c =$
370 7300s in Fig. 6a). The model predicts that the 3 calcium signatures shown in Fig. 1 would
371 generally generate small fold changes for *EDS1* expression (Fig. 6b,f). Our experimental data
372 indeed confirmed that the three calcium signatures always generate small transcript fold
373 changes for *EDS1* gene expression (around maximum 3 fold at 1 hour, Fig. 6b,f). The model
374 also correctly predicted that the calcium signature triggered by glutamate (Fig. 1) would not
375 induce *EDS1* expression at all, which was confirmed by experimental observation (Fig. 6d).
376 Therefore, modelling predictions for both *EDS1* and *ICS1* expression are in agreement with
377 experimental observations.

378 Additionally, the model was able to predict the temporal trends of the transcript fold
379 responses for both *EDS1* and *ICS1* gene expression to the three test calcium signatures.
380 Experimental data show that fold change of *EDS1* expression from 1 hour to 9 hours
381 generally does not display temporal variation (Fig. 6b,d,f) for the three calcium signatures.
382 The model correctly predicts that *EDS1* expression for the three calcium signatures generally
383 does not change temporally from 1 hour to 9 hours (Fig. 6b,d,f). Experimental data show
384 that the calcium signatures induced by both ATP and glutamate result in *ICS1* transcript fold
385 change generally decreasing from 1 hour to 9 hours (Fig. 6c,e) whereas the calcium
386 signature induced by extracellular Ca^{2+} results in *ICS1* transcript fold change generally
387 increasing from 1 hour to 9 hours (Fig. 6a). Again, the model was able to predict similar
388 temporal *ICS1* transcript fold change trends for the 3 test calcium signatures (Fig. 6a,c,e).
389 Taken together, the model (Fig. 3) was thus able to correctly predict the temporal trends of
390 the transcript fold responses for both *EDS1* and *ICS1* gene expression to the three test
391 calcium signatures. Therefore, our results have demonstrated that a novel integrated
392 experimental and modelling study, in which a wide range of biological knowledge in the
393 literature is integrated with our own experimental data, can elucidate and predict the
394 response of *EDS1* and *ICS1* gene expression to different calcium signatures.

395

396 **Discussion**

397 Here we describe a novel integrated experimental and modelling study, in which a wide
398 range of biological knowledge from the literature was integrated with our experimental
399 data. This enabled us to establish the information flow from calcium signatures to the
400 expression of specific calcium-regulated genes in plant cells. Our experimental data show
401 that different calcium signatures can generate specific *EDS1* and *ICS1* gene expression
402 responses (Fig. 2 and 6). The biological knowledge accumulated over many years in the
403 literature was abstracted into a dynamic model (Fig. 3). The model was parameterised by
404 using experimentally measured parameters in the literature (Liu *et al.*, 2015) and by fitting
405 the model to the experimentally measured transcript fold changes for both *EDS1* and *ICS1*
406 genes in response to the calcium signature induced by 10 μ M mastoparan (Fig. 1). We
407 further demonstrated that the model developed in this study was always able not only to
408 reproduce experimental observations (Fig. 4, 6, S1, S2 and S3), but also to make predictions
409 that are validated experimentally (Fig. 6, S4, S5, S6). Therefore, a combined experimental
410 and modelling study is able to reveal how different calcium signatures are decoded to
411 specific responses gene expression. Relationships between calcium signatures and
412 responses of *EDS1* and *ICS1* gene expression can therefore be elucidated and predicted. Our
413 work also establishes how calcium signatures are decoded by Arabidopsis to generate the
414 expression responses of two genes (*EDS1* and *ICS1*) important in plant immunity. Our
415 combined modelling and experimental analysis reveals the complexity of this decoding
416 process. Calcium signals are amplified into three active signals via Ca^{2+} and CaM interaction,
417 and via both CAMTA3 and CBP60g transcription factors (the 3 signals being: 4Ca^{2+} -CaM,
418 4Ca^{2+} -CaM-CAMTA3 and 4Ca^{2+} -CaM-CBP60g). In addition, since expression of *EDS1* and *ICS1*
419 forms a network (Fig. 3), the three active signals, which originate from the same calcium
420 signature, interplay via this network. Thus, regulation of *EDS1* and *ICS1* expression (Fig. 2, 5
421 and 6) by the calcium signatures is highly nonlinear due to the interactions of these three
422 amplified active signals (Fig. 4b,c,d). Therefore, specific responses of *EDS1* and *ICS1*
423 expression to the calcium signatures are due to nonlinear interactions of the three amplified
424 active signals originating from the same calcium signature. Because our combined
425 experimental and modelling study is able to establish the relationships between gene
426 expression responses and calcium signatures, it supports the concept that calcium signalling
427 plays a vital role in plant immunity.

428 Calcium signatures are generally relatively short lived increases in calcium
429 concentration. As a dynamically transient signal, a calcium signature generally tends to
430 return to a steady state level. This level can be the same concentration as before the start of
431 the transient, or can be a different steady state level. Traditionally, much attention has
432 been paid to the characteristics of a calcium signature within a relatively short period after
433 initiation. How a calcium signature returns to a steady state has been largely ignored. Our
434 work shows that the time required for a calcium signature to return to a steady state, τ_c , is
435 a factor which quantitatively affects the subsequent gene expression response. This
436 demonstrates that our combined experimental and modelling methodology is capable of
437 identifying unknown factors about the decoding of calcium signatures. As the key properties
438 of the calcium signatures important in mediating specific gene expression responses were
439 not intuitive this necessitated a mathematical modelling approach.

440 Whilst our combined experimental and modelling methodology is capable of
441 predicting both the fold change and temporal pattern for *EDS1* and *ICS1* gene expression
442 (Fig. 5 and 6), our model (Fig. 3) cannot perfectly fit the expression pattern of *EDS1* and *ICS1*
443 for agonist mastoparan (Fig. 5) nor perfectly predict the expression pattern of both genes
444 for other agonists (Fig. 6). For example, whilst Fig. 5 shows that *ICS1* gene expression for
445 agonist mastoparan is induced at 3600s according to experimental measurements, the
446 computed fold change of *ICS1* transcripts does not increase until 5200s. Once the time
447 reaches 5200s, the fold change starts to rapidly increase in the model fitting. When a
448 calcium signal is produced, a change in gene expression cannot occur instantaneously, as
449 the transcriptional pre-initiation complex (containing specific transcription factors e.g.
450 CAMTA3, general transcription factors, mediator and RNA polymerase) needs to be
451 recruited and assembled and an elongation complex needs to form to allow transcription
452 of the coding region (Lee and Young, 2000). Therefore, a time delay between calcium signal
453 and gene expression response needs to be considered (Liu et al., 2015). Since the exact
454 subcellular locations of both Ca^{2+} and the components for both *EDS1* and *ICS1* expression
455 such as transcription factor, Mediator and RNA polymerase have not been experimentally
456 determined, a single parameter, included in Table S1, is used to describe the time delay
457 between calcium signal and gene expression response. Fig. S7 shows that increasing the
458 time delay of either *ICS1* or *EDS1* gene expression increases the induction time of *ICS1* or

459 *EDS1* gene expression accordingly. For example, increasing the time delay of *ICS1* from
460 3600s to 7200s increases the induction time of *ICS1* gene expression from 3600s to 7200s.
461 Fig. S8 shows that a time delay between 5000s and 9000s for *ICS1* gene expression
462 generates best-fitting of the fold changes of *ICS1* transcripts. However, a time delay
463 between 200s and 1000s for *EDS1* gene expression generates best-fitting of the fold
464 changes of *ICS1* transcripts. Therefore, together Fig. S7 and S8 reveals that time delay is an
465 important parameter for determining when *EDS1* and *ICS1* expression is induced. Although
466 time delay can affect modelling results, we have not found such a combination of the two
467 time delays for *EDS1* and *ICS1* expression that a perfect fitting or prediction can be
468 generated. Since time delay between calcium signal and gene expression response is
469 defined by a single parameter, once time delay has elapsed, gene expression immediately
470 starts to rapidly increase (Fig. 5) following a rapid increase in calcium concentration at the
471 beginning of a calcium signature (Fig. 1). However, it is plausible that the availability of the
472 components required for gene expression such as transcription factors, Mediator and RNA
473 polymerase at the location of gene expression is also important for gene expression
474 response. Thus, to improve model fitting and prediction, the model (Fig. 3) needs to be
475 further developed to include the exact subcellular locations of Ca^{2+} and the components for
476 gene expression such as transcription factor, Mediator and RNA polymerase. However,
477 constructing a model to explicitly include spatial setting is currently impossible as such
478 experimental data are unavailable. Recently, Yuan et al. (2017) discussed that detection of
479 the exact subcellular locations of Ca^{2+} is important for future research. Combining a high
480 resolution of spatial Ca^{2+} distribution with experimentally-measured locations of
481 components required for the expression of *EDS1* and *ICS1* such as transcription factors,
482 Mediator and RNA polymerase, future research should be able to more precisely predict the
483 dynamics of gene expression.

484 Experimental data accumulated over many years have revealed multiple levels of
485 complexities in decoding calcium signals in plant cells (Edel et al. 2017; Yuan et al. 2017).
486 Plants cells possess four main types of Ca^{2+} sensor proteins to relay or decode Ca^{2+}
487 signalling: CaM, CaM-like proteins (CMLs), calcineurin B-like proteins (CBLs) and Ca^{2+} -
488 dependent protein kinases (CDPKs or CPKs) (Yuan et al. 2017). These proteins relay or
489 decode calcium signals at both transcriptional and post-translational levels (Yuan et al.
490 2017). Our research presented in this work has focused on an example at the transcriptional

491 level specifically. Using two important genes in plant immunity, *EDS1* and *ICS1*, as an
492 example, this work demonstrates that the specific responses of gene expression to calcium
493 signatures can be elucidated and predicted by a combined experimental and modelling
494 analysis and that a cellular mechanism for decoding calcium signatures can be identified
495 (Fig. 3). In principle, the upper pane of Fig. 3 could be used to study the interactions of Ca^{2+}
496 and any Ca^{2+} and/or CaM binding protein. For example, during symbiosis, the Ca^{2+} /CaM-
497 dependent protein kinase (CCaMK) (Gleason et al. 2006; Patil et al 1995) plays an essential
498 role in the interpretation of symbiotic Ca^{2+} signalling in the nucleus for the establishment of
499 symbiotic responses (Yuan et al. 2017). Thus, to explore symbiotic responses, CCaMK could
500 be explicitly included in the upper pane of Fig. 3 to investigate how CCaMK interacts with
501 Ca^{2+} and calmodulin to generate an active signal for promoting the phosphorylation of a
502 substrate. Similarly, in principle, the lower pane of Fig. 3 can be used to study the regulation
503 of any biological system by any active Ca^{2+} signal. For example, the active signal generated
504 by the interaction of Ca^{2+} , CaM and CCaMK, which can be computed after incorporating
505 CCaMK into the upper pane of Fig. 3, can be used to investigate how CCaMK promotes the
506 phosphorylation of a substrate if the regulatory mechanism of the phosphorylation process
507 can be established the lower pane of Fig. 3 following experimental data. In addition, it is also
508 possible to study the interplay between the post-translational level and transcriptional level,
509 e.g. by establishing how CCaMK, CAMTA3 and CBP60g compete for the binding with CaM.
510 Thus, the methodology developed here can be further developed to study the decoding of
511 calcium signatures in both transcriptional and post-translational levels, and to determine
512 the decoding mechanisms of calcium signatures at both levels in plant cells.

513

514 **Acknowledgements**

515 This work was funded by an EU-funded Initial Training Network (ITN) CALIPSO GA 2013–
516 607607.

517 **Author contributions**

518 G.L., J.L. and M.R.K. designed the experiments and the model, analysed the data and wrote
519 the paper; G.L. conducted the experiments; J.L. developed modelling analysis.

520

521 **References**

522 **Allen GJ, Chu SP, Harrington CL, Schumacher K, Hoffmann T, Tang YY, Grill E, Schroeder JI. 2001.** A
523 defined range of guard cell calcium oscillation parameters encodes stomatal movements.
524 *Nature* **411**: 1053-1057.

525 **Berridge MJ, Bootman MD, Roderick HL. 2003.** Calcium signalling: Dynamics, homeostasis and
526 remodelling. *Nature Reviews Molecular Cell Biology* **4**: 517-529.

527 **Bickerton PD, Pittman JK 2012.** Calcium Signalling in Plants. *eLS*: John Wiley & Sons, Ltd.,
528 Chichester.

529 **Clapham DE. 2007.** Calcium signaling. *Cell* **131**: 1047-1058.

530 **Dodd AN, Kudla J, Sanders D. 2010.** The language of calcium signaling. *Annu Rev Plant Biol* **61**: 593-
531 620.

532 **Du L, Ali GS, Simons KA, Hou J, Yang T, Reddy ASN, Poovaiah BW. 2009.** Ca²⁺/calmodulin regulates
533 salicylic-acid-mediated plant immunity. *Nature* **457**: 1154-1158.

534 **Edel KH, Marchadier E, Brownlee C, Kudla J, Hetherington AM. 2017.** The evolution of calcium-
535 based signalling in plants. *Current Biology* **27**: R667-R679.

536 **Finkler A, Ashery-Padan R, Fromm H. 2007.** CAMTAs: calmodulin-binding transcription activators
537 from plants to human. *FEBS Lett* **581**: 3893-3898.

538 **Galon Y, Aloni R, Nachmias D, Snir O, Feldmesser E, Scrase-Field S, Boyce JM, Bouche N, Knight**
539 **MR, Fromm H. 2010.** Calmodulin-binding transcription activator 1 mediates auxin signaling
540 and responds to stresses in Arabidopsis. *Planta* **232**: 165-178.

541 **Gleason C, Chaudhuri S, Yang T, Munoz A, Poovaiah BW, Oldroyd GED. 2006.** Nodulation
542 independent of rhizobia induced by a calcium-activated kinase lacking autoinhibition. *Nature*
543 **441**: 1149-1152.

544 **Galon Y, Nave R, Boyce JM, Nachmias D, Knight MR, Fromm H. 2008.** Calmodulin-binding
545 transcription activator (CAMTA) 3 mediates biotic defense responses in Arabidopsis. *FEBS*
546 *Lett* **582**: 943-948.

547 **Grant M, Brown I, Adams S, Knight M, Ainslie A, Mansfield J. 2000.** The RPM1 plant disease
548 resistance gene facilitates a rapid and sustained increase in cytosolic calcium that is
549 necessary for the oxidative burst and hypersensitive cell death. *Plant Journal* **23**: 441-450.

550 **Hashimoto K, Kudla J. 2011.** Calcium decoding mechanisms in plants. *Biochimie* **93**: 2054-2059.

551 **Kim MC, Chung WS, Yun DJ, Cho MJ. 2009.** Calcium and calmodulin-mediated regulation of gene
552 expression in plants. *Mol Plant* **2**: 13-21.

553 **Kim MC, Panstruga R, Elliott C, Muller J, Devoto A, Yoon HW, Park HC, Cho MJ, Schulze-Lefert P.**
554 **2002.** Calmodulin interacts with MLO protein to regulate defence against mildew in barley.
555 *Nature* **416**: 447-451.

556 **Knight H, Knight MR. 1995.** Recombinant aequorin methods for intracellular calcium measurement
557 in plants. *Methods Cell Biol* **49**: 201-216.

558 **Knight H, Mugford SG, Ulker B, Gao D, Thorlby G, Knight MR. 2009.** Identification of SFR6, a key
559 component in cold acclimation acting post-translationally on CBF function. *Plant J* **58**: 97-
560 108.

561 **Knight H, Trewavas AJ, Knight MR. 1996.** Cold calcium signaling in Arabidopsis involves two cellular
562 pools and a change in calcium signature after acclimation. *Plant Cell* **8**: 489-503.

563 **Knight MR, Campbell AK, Smith SM, Trewavas AJ. 1991.** Transgenic Plant Aequorin Reports the
564 Effects of Touch and Cold-Shock and Elicitors on Cytoplasmic Calcium. *Nature* **352**: 524-526.

565 **Kudla J, Batistic O, Hashimoto K. 2010.** Calcium signals: the lead currency of plant information
566 processing. *Plant Cell* **22**: 541-563.

567 **Lee TI, Young RA. 2000.** Transcription of eukaryotic protein-coding genes. *Annual Review of Genetics*
568 **34**: 77-137.

569 **Liu J, Whalley HJ, Knight MR. 2015.** Combining modelling and experimental approaches to explain
570 how calcium signatures are decoded by calmodulin-binding transcription activators
571 (CAMTAs) to produce specific gene expression responses. *New Phytol.* **208**: 174-187.

572 **Livak KJ, Schmittgen TD. 2001.** Analysis of relative gene expression data using real-time quantitative
573 PCR and the $2^{-\Delta\Delta C(T)}$ Method. *Methods* **25**: 402-408.

574 **McAinsh MR, Pittman JK. 2009.** Shaping the calcium signature. *New Phytol* **181**: 275-294.

575 **Murashige T, Skoog F. 1962.** A Revised Medium for Rapid Growth and Bio Assays with Tobacco
576 Tissue Cultures. *Physiol Plant* **15**: 473-497.

577 **Patil S, Takezawa D, Poovaiah BW. 1995.** Chimeric plant calcium/ calmodulin-dependent protein
578 kinase gene with a neural visinin-like calcium-binding domain. *Proceedings of the National*
579 *Academy of Sciences* **92**: 4897-4901.

580 **Piffl C, Plank B, Wiskovsky W, Bertel O, Hellmann G, Suko J. 1984.** Calmodulin X (Ca²⁺)₄ is the active
581 calmodulin-calcium species activating the calcium-, calmodulin-dependent protein kinase of
582 cardiac sarcoplasmic reticulum in the regulation of the calcium pump. *Biochim Biophys Acta*
583 **773**: 197-206.

584 **Poovaiah BW, Du L, Wang H, Yang T. 2013.** Recent Advances in Calcium/Calmodulin-Mediated
585 Signaling with an Emphasis on Plant-Microbe Interactions. *Plant Physiol* **163**: 531-542.

586 **Ranty B, Aldon D, Cotellet V, Galaud JP, Thuleau P, Mazars C. 2016.** Calcium Sensors as Key Hubs in
587 Plant Responses to Biotic and Abiotic Stresses. *Frontiers in Plant Science* **7**, 1-7.

588 **Reddy AS, Ali GS, Celesnik H, Day IS. 2011.** Coping with stresses: roles of calcium- and
589 calcium/calmodulin-regulated gene expression. *Plant Cell* **23**: 2010-2032.

590 **Seybold H, Trempel F, Ranf S, Scheel D, Romeis T, Lee J. 2014.** Ca²⁺ signalling in plant immune
591 response: from pattern recognition receptors to Ca²⁺ decoding mechanisms. *New Phytol*
592 **204**: 782-790.

593 **Tsuda K, Somssich IE. 2015.** Transcriptional networks in plant immunity. *New Phytol* **206**: 932-947.

594 **Vlot AC, Dempsey DA, Klessig DF. 2009.** Salicylic Acid, a multifaceted hormone to combat disease.
595 *Annu Rev Phytopathol* **47**: 177-206.

596 **Wang L, Tsuda K, Sato M, Cohen JD, Katagiri F, Glazebrook J. 2009.** Arabidopsis CaM binding protein
597 CBP60g contributes to MAMP-induced SA accumulation and is involved in disease resistance
598 against *Pseudomonas syringae*. *PLoS Pathog* **5**: e1000301.

599 **Wang L, Tsuda K, Truman W, Sato M, Nguyen le V, Katagiri F, Glazebrook J. 2011.** CBP60g and
600 SARD1 play partially redundant critical roles in salicylic acid signaling. *Plant J* **67**: 1029-1041.

601 **Whalley HJ, Knight MR. 2013.** Calcium signatures are decoded by plants to give specific gene
602 responses. *New Phytol* **197**: 690-693.

603 **Yuan P, Jauregui E, Du L, Tanaka K, Poovaiah BW. 2017** Calcium signatures and signaling events
604 orchestrate plant-microbe interactions. *Curr Opin Plant Biol.* **38**: 173-183.

605 **Zhang L, Du L, Shen C, Yang Y, Poovaiah BW. 2014.** Regulation of plant immunity through ubiquitin-
606 mediated modulation of Ca(2+) -calmodulin-AtSR1/CAMTA3 signaling. *Plant J* **78**: 269-281.

607 **Zhang Y, Xu S, Ding P, Wang D, Cheng YT, He J, Gao M, Xu F, Li Y, Zhu Z, Li X, Zhang Y. 2010.** Control
608 of salicylic acid synthesis and systemic acquired resistance by two members of a plant-
609 specific family of transcription factors. *Proceedings of the National Academy of Sciences* **107**:
610 18220-18225.

611 **Zipfel C, Oldroyd GED. 2017.** Plant signalling in symbiosis and immunity. *Nature* **543**: 328-336.

612

613 **Figure legends**

614 **Fig. 1** Different calcium agonists produce different calcium signatures. Effect upon cytosolic
615 calcium concentration ($[Ca^{2+}]_c$) in *Arabidopsis thaliana* of treatment with either 500 μ M ATP
616 (ATP); 50 mM extracellular calcium (eCa); 1 mM glutamate (L-Glu); or 10 μ M mastoparan.
617 (a) $[Ca^{2+}]_c$ plotted against 1000s, shading around each plot line represents standard error of
618 the mean (n=6 replicates of 5 treated seedlings); (b) $[Ca^{2+}]_c$ plotted against 110-160s to
619 show details of early kinetics in $[Ca^{2+}]_c$, error bars represents standard error of the mean
620 (n=6 replicates of 5 treated seedlings).

621 **Fig. 2** Calcium signature in response to mastoparan induces *ICS1* and *EDS1* gene expression.
622 (a) Fold increase in *ICS1* transcript expression in *Arabidopsis thaliana* in response to 10 μ M
623 mastoparan 1, 3, 6 and 9h after start of treatment. (b) Fold increase in *EDS1* transcript
624 expression in *Arabidopsis thaliana* in response to 10 μ M mastoparan 1, 3, 6 and 9h after
625 start of treatment. Letters above error bars refer to significant difference ($P < 0.05$) between
626 the average CT values for each timepoint/treatment as determined by pairwise t-tests.
627 Below these letters are symbols to denote the significant difference in average CT value
628 compare to baseline expression at that timepoint; $P < 0.0005$ (*****), $P < 0.005$ (***), $P < 0.05$
629 (*), not significant (ns) as determined by pairwise t-tests.

630 **Fig. 3** A dynamic model for the information flow from calcium signatures to *EDS1* and *ICS1*
631 gene expression. The upper pane describes the interactions of Ca^{2+} , CaM, CAMTA3, CBP60g
632 and other CaM-binding proteins. The interactions of Ca^{2+} -CaM and CAMTA3 have been
633 previously described in detail (Liu et al., 2015). Other interactions are dealt with in the same
634 way as for the interactions of Ca^{2+} -CaM and CAMTA3 (See "A dynamic model for the
635 information flow from calcium signals to gene expression" section). The lower pane
636 describes the regulatory network of *EDS1* and *ICS1* expression (Zhang et al., 2014). We
637 simplified the network downstream of *ICS1* into a single component, downstream response
638 (DR). Black solid lines: mass conversion; red solid lines: regulatory relationships confirmed
639 by experiments; red dash lines: regulatory relationships derived from experiments.

640 **Fig. 4** Dynamic model-fitting to experimental data for calcium signature and gene expression
641 responses to mastoparan. (a) Calcium signature induced by 10 μ M mastoparan and how it
642 approaches its steady state. (b) Response of active signal $4Ca^{2+}$ -CaM to the calcium
643 signature (MNNCC_: M: CaM; N: 1 Ca^{2+} binding to N-terminus of CaM; C: 1 Ca^{2+} binding to C-
644 terminus of CaM; _: no binding – the regulation of *EDS1* expression by the network
645 upstream of it is assumed to be via an active Ca^{2+} signal ($4Ca^{2+}$ -CaM)). (c) Response of active
646 signal $4Ca^{2+}$ -CaM-CAMTA3 to the calcium signature (MNNCCX: M: CaM; N: 1 Ca^{2+} binding to
647 N-terminus of CaM; C: 1 Ca^{2+} binding to C-terminus of CaM; X: CAMTA3). (d) Response of
648 active signal $4Ca^{2+}$ -CaM-CBP60g to the calcium signature (MNNCCY: M: CaM; N: 1 Ca^{2+}
649 binding to N-terminus of CaM; C: 1 Ca^{2+} binding to C-terminus of CaM; Y: CBP60g). From left
650 to right (i.e. the curve with the colour dark blue, red, green, brown and light blue,

651 respectively) : $\tau_c = 1000s, 3700s, 7300s, 11800s, 15400s$, respectively (τ_c is the time
652 required for transient elevation of calcium concentration to re-establish a steady state).
653 Parameters are included in Table S1.

654 **Fig 5.** Comparison of modelled gene expression with experimental data. (a) Comparison of
655 modelled fold changes of *EDS1* transcript with experimental data from *Arabidopsis thaliana*.
656 Curves are the modelling results and the scattered data with error bars are the experimental
657 results. (b) Comparison of modelled fold changes of *ICS1* transcript with experimental data
658 from *Arabidopsis thaliana*. Curves are the modelling results and the scattered data with
659 error bars are the experimental results. Each sub-graph has 5 curves, corresponding to
660 different values of τ_c (the time required for transient elevation of calcium concentration to
661 re-establish a steady state). From bottom to top (i.e. the curve with the colour dark blue,
662 red, green, brown and light blue, respectively): $\tau_c = 1000s, 3700s, 7300s, 11800s, 15400s$,
663 respectively. Parameters are included in Table S1.

664 **Fig. 6** Modelling predictions on the transcript fold responses for both *EDS1* and *ICS1* to three
665 calcium signatures and their comparison with experimental observations. (a) to (f) are
666 modelling predictions and their comparison with experimental observations from
667 *Arabidopsis thaliana*. (a) Predicted fold change of *ICS1* transcripts over time in response to
668 the calcium signature induced by extracellular calcium. (b) Predicted fold change of *EDS1*
669 transcripts over time in response to the calcium signature induced by extracellular calcium.
670 (c) Predicted fold change of *ICS1* transcripts over time in response to the calcium signature
671 induced by glutamate. (d) Predicted fold change of *EDS1* transcripts over time in response to
672 the calcium signature induced by glutamate. (e) Predicted fold change of *ICS1* transcripts
673 over time in response to the calcium signature induced by ATP. (f) Predicted fold change of
674 *EDS1* transcripts over time in response to the calcium signature induced by ATP. In (a) to (f)
675 curves are the modelling results and the scattered data with error bars are the experimental
676 results. Letters above error bars refer to significant difference ($P < 0.05$) between the average
677 CT values for each timepoint/treatment as determined by pairwise t-tests. Below these
678 letters are symbols to denote the significant difference in average CT value compare to
679 baseline expression at that timepoint; $P < 0.0005$ (*****), $P < 0.001$ (****), $P < 0.005$ (***),
680 $P < 0.01$ (**), $P < 0.05$ (*), not significant (ns) as determined by pairwise t-tests. In (a) to (f)

681 each sub-graph has 5 curves, corresponding to different values of τ_c (the time required for
682 transient elevation of calcium concentration to re-establish a steady state). From bottom to
683 top (i.e. the curve with the colour dark blue, red, green, brown and light blue, respectively):
684 $\tau_c = 1000s, 3700s, 7300s, 11800s, 15400s$, respectively. Parameters are the same as in Fig. 4
685 and 5, and they are included in Table S1.

686 **Fig. S1** Comparison of modelled gene expression with experimental data with altered
687 parameters described in Table S1.

688 **Fig. S2** Comparison of modelled gene expression with experimental data with altered
689 parameters described in Table S1.

690 **Fig. S3** Comparison of modelled gene expression with experimental data with altered
691 parameters described in Table S1.

692 **Fig. S4** Modelling predictions on the transcript fold responses for both *EDS1* and *ICS1* with
693 altered parameters described in Table S1.

694 **Fig. S5** Modelling predictions on the transcript fold responses for both *EDS1* and *ICS1* with
695 altered parameters described in Table S1.

696 **Fig. S6** Modelling predictions on the transcript fold responses for both *EDS1* and *ICS1* with
697 altered parameters described in Table S1.

698 **Fig. S7** Effects of the time delay between calcium signal and gene expression response on
699 the dynamics of the fold changes of gene expression.

700 **Fig. S8** Dependence of the difference between the experimental fold change of both *ICS1*
701 and *EDS1* transcripts and the computed counterparts on the delay time between calcium
702 signal and gene expression response.

703 **Table S1** Parameters for modelling and parameter searching.

704 **Table S2** Original code (program) for the modelling analysis.

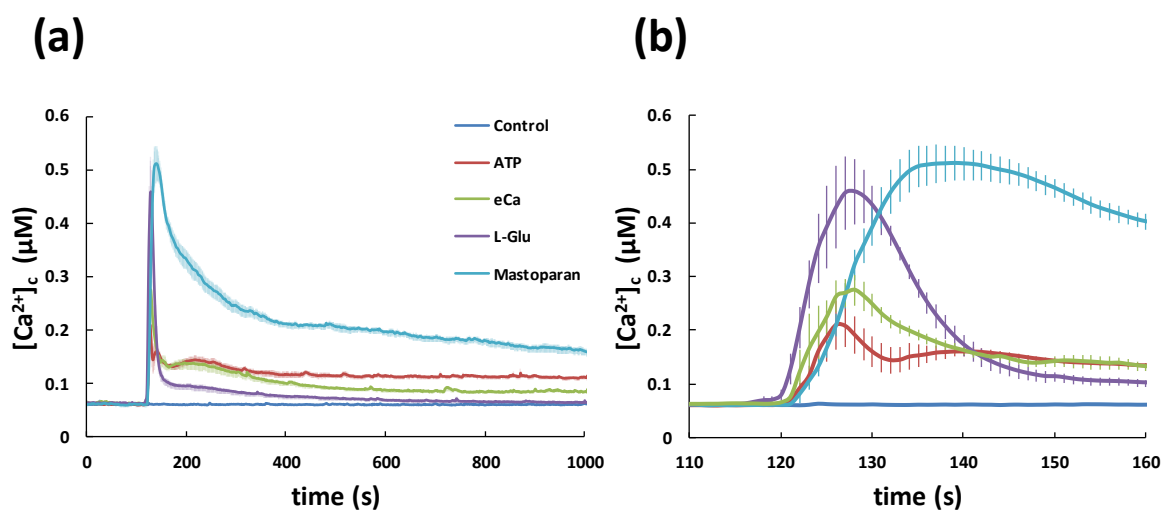


FIGURE 1

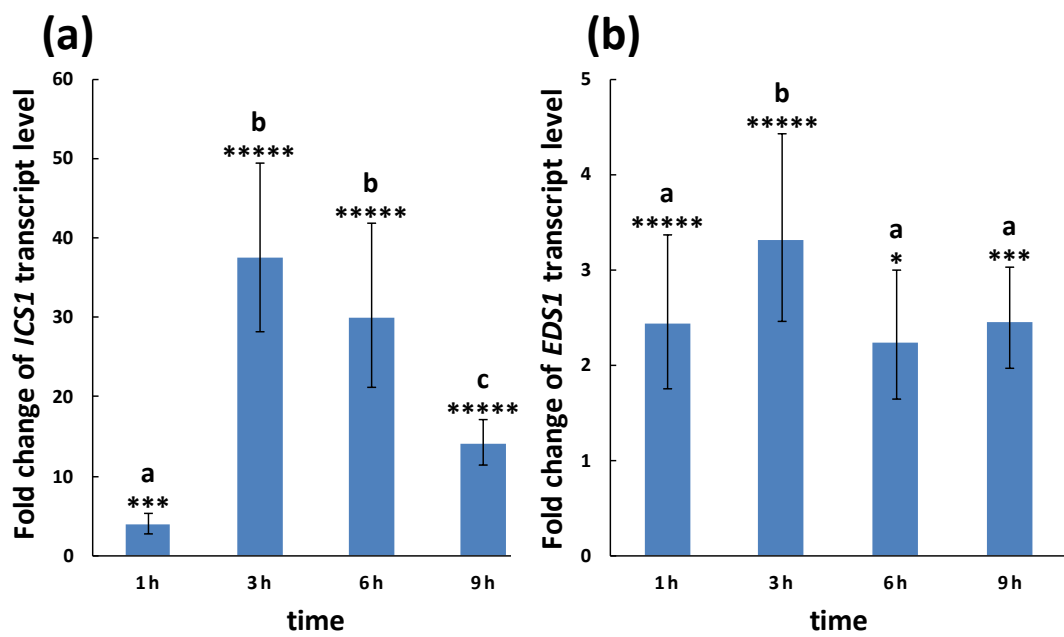


FIGURE 2

Interactions between Ca^{2+} , CaM, CAMTA3, CBP60g and other CaM-binding proteins

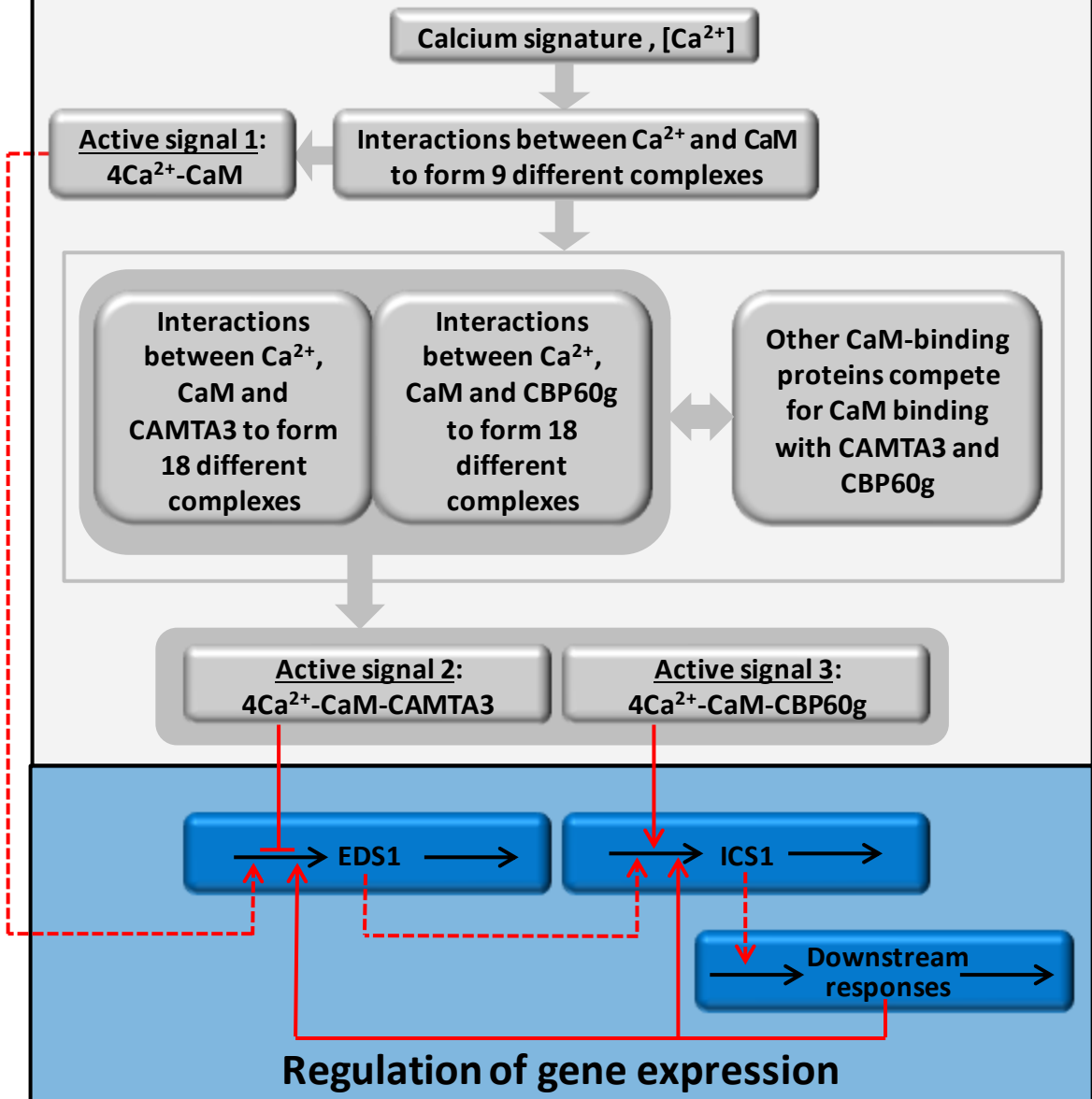


FIGURE 3

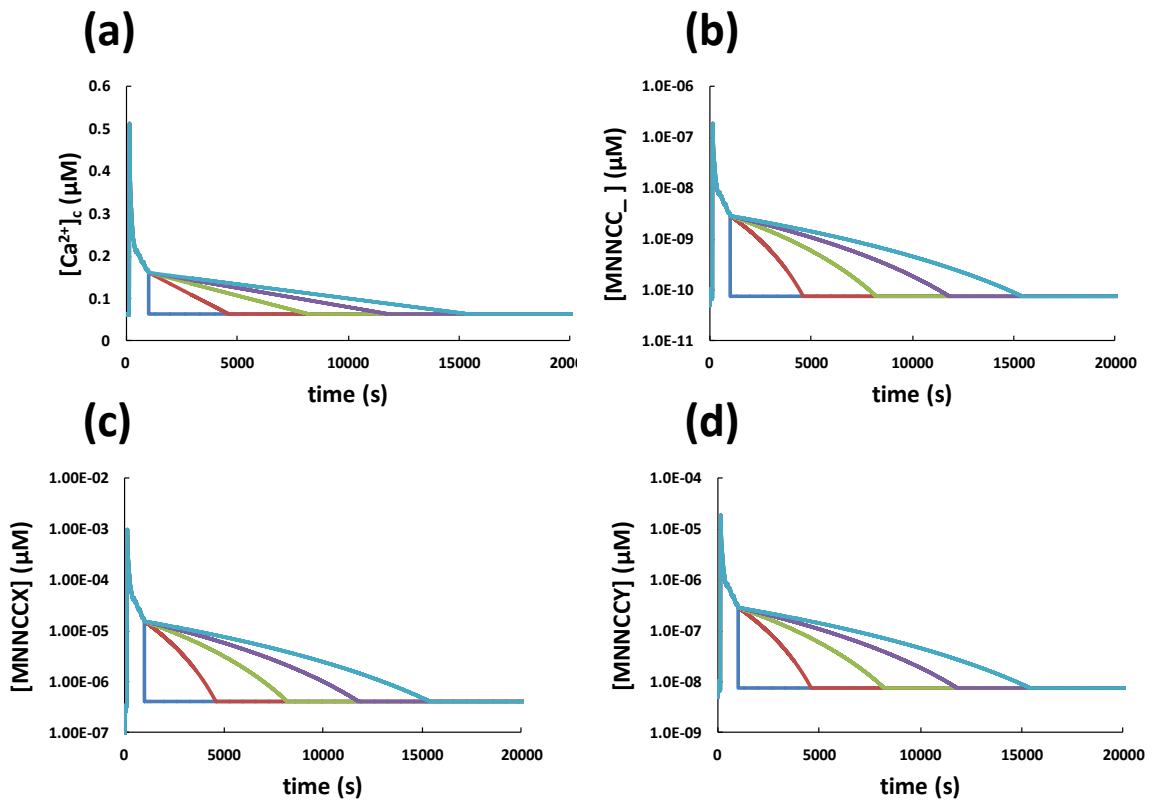


FIGURE 4

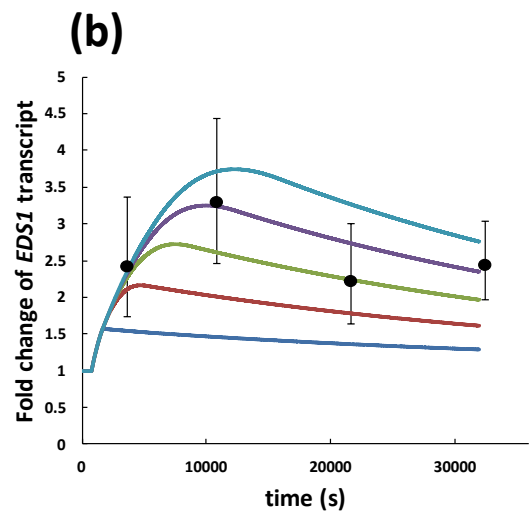
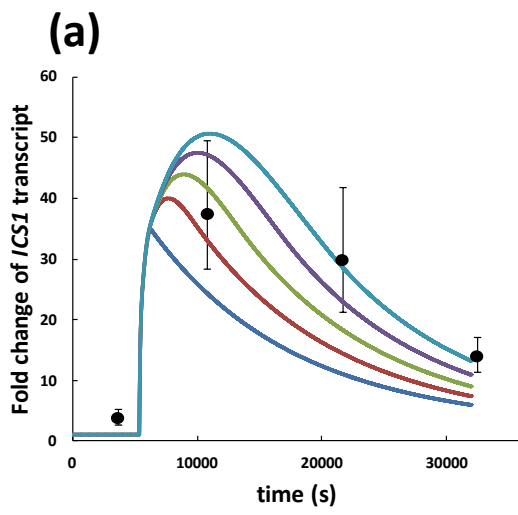


FIGURE 5

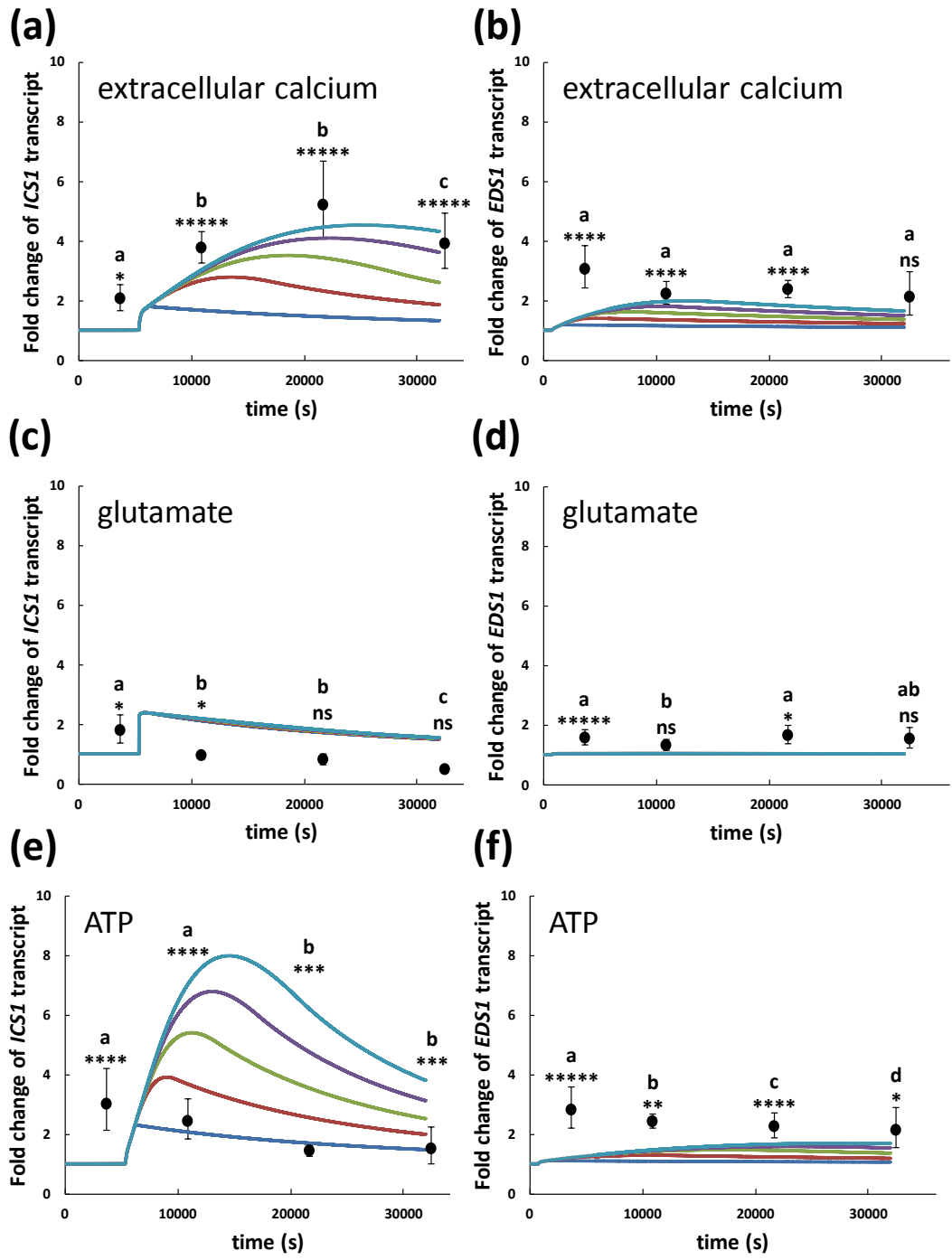


FIGURE 6